Acta Oceanol. Sin., 2019, Vol. 38, No. 10, P. 93–99
https://doi.org/10.1007/s13131-019-1482-7
http://www.hyxb.org.cn
E-mail: hyxbe@263.net

An improved ARTSIST sea ice algorithm based on 19 GHz modified 91 GHz

Zhankai Wu[1], Xingdong Wang[1, 2]*, Xuemei Wang[1]

[1] College of Information Science and Engineering, Henan University of Technology, Zhengzhou 450001, China

[2] Institute of Remote Sensing and Digital Earth, Chinese Academy of Sciences, Beijing 100094, China

Received 19 June 2018; accepted 29 September 2018

Abstract

An enhanced ARTSIST Sea Ice (ASI) algorithm is presented based on a data fusion method of calculating total sea ice concentration from high-frequency microwave data. Algorithms that use low-frequency data to calculate total sea ice concentration are less affected by atmosphere, but their spatial resolutions tend to be lower. In contrast, algorithms using high-frequency data have higher spatial resolution but are significantly influenced by atmosphere. Although errors can be eliminated using weather filters, the concentration of mixed pixels cannot be modified. Here, an enhanced ASI algorithm uses the 19 GHz polarization difference to modify the 91 GHz polarization difference, which is substituted into the ASI algorithm to calculate total sea ice concentration. Arctic total sea ice concentration results are obtained based on Special Sensor Microwave Imager Sounder (SSMIS) data on January 3, from 2008 to 2017. Total sea ice area and average concentration using the enhanced ASI algorithm are compared to traditional ASI and NASA Team results. In the Marginal Ice Zone, there is a considerable difference between the enhanced and traditional ASI algorithm results, with the former much closer to the NASA Team results. The proposed algorithm effectively modifies the concentration of the mixed pixels in the marginal zone.

Key words: ASI algorithm, sea ice concentration, SSMIS, NASA Team algorithm

Citation: Wu Zhankai, Wang Xingdong, Wang Xuemei. 2019. An improved ARTSIST sea ice algorithm based on 19 GHz modified 91 GHz. Acta Oceanologica Sinica, 38(10): 93–99, doi: 10.1007/s13131-019-1482-7

1 Introduction

Sea ice concentration describes the area covered by sea ice in space. It is one of the most important parameters describing sea ice characteristics when studying atmospheric and ocean circulation patterns. Furthermore, sea ice concentration has an important impact on the heat flux between the ocean and atmosphere (Schmidtko et al., 2014). Changing Arctic sea ice is recognized as one of the most important measurement indices among those in the Arctic climate system (Budikova, 2009). Sea ice affects earth ecosystem and is the biggest obstacle to developing the Arctic channel (Spreen et al., 2008).

Andersen et al. (2007) summarized seven sea ice concentration retrieval algorithms designed for SSM/I data. NASA Team is a widespread algorithm for calculating first-year and multiyear ice concentrations (Swift and Cavalieri, 1985) and the Bootstrap algorithm, based on the basic radiative transfer equation, is also used to calculate total sea ice concentration (Comiso, 1986, 1995). The NASA-Team2 (Markus and Cavalieri, 2000), SEA LION (Kern and Heygster, 2001), and ASI (Kaleschke, et al., 2001) algorithms include Special Sensor Microwave/Imager (SSM/I) 85 GHz band data, and they can provide 12.5 km resolution sea ice concentration grid data. The ASI algorithm was developed in 1998 as part of the "Arctic Radiation and Turbulent Exchange Study". It is based on the concept of "polarization-corrected temperature" (Spencer et al., 1989) and uses data near the 90 GHz band to calculate sea ice concentration (Svendsen et al., 1987). At the outset, the ASI algorithm was only used to conduct mid-scale numerical simulations of the atmospheric boundary layer at the Arctic sea ice edge using higher resolution SSM/I 85 GHz data (Kaleschke et al., 2001). Zhang (2012) derived a sea ice concentration algorithm called the dual-polarized ratio (DPR) method, which is independent of sea ice microwave emissivity. Wang (2009) proposed a method for calculating multi-year ice concentrations based on different characteristics between first-year ice, multiyear ice, and sea water in the 89 GHz band. Su et al. (2013) implemented a series of experiments, including interpolation algorithm "tie-points" and a weather filter, based on the ASI algorithm. Zhang et al. (2012) proposed a method that uses many bands and dual-polarization to calculate sea ice concentration depending on the characteristics of sea ice and seawater radiation.

Kern et al. (2016) analyzed the influence of molten pool on the summer microwave brightness temperature data and sea ice concentration, and then improved the inversion accuracy of sea ice concentration. Korosov et al. (2018) proposed an algorithm based on Euler advection scheme to estimate the distribution of sea ice at different ice ages. Gabarro et al. (2017) proposed a new method for estimating Arctic sea ice concentration using maxim-

Foundation item: The National Natural Science Foundation of China under contract No. 41606209; the Open Fund from Key Laboratory of Global Change and Marine-Atmospheric Chemistry under contract No. GCMAC1605; the Natural Science Project of Henan Education Department under contract No. 15A120007; the Key Laboratory of Ocean Circulation and Waves, Institute of Oceanology, Chinese Academy of Sciences under contract No. KLOCW1805.
*Corresponding author, E-mail: zkywxd@163.com

um likelihood estimation combined with SMOS of luminance temperature difference. Ye et al. (2016) by introducing the analysis of air temperature data, improve the accuracy of sea ice concentration inversion result.

Although the ASI algorithm had advantages, compared with the low frequency data, the 89 GHz band data is more influenced by atmospheric cloud liquid water, rain droplets, water vapor, and snow particle density on the ice surface; therefore, weather filter processing is needed in the ASI algorithm (Spreen et al., 2008). Although some errors can be eliminated using weather filters, the concentration of mixed pixels cannot be modified. To achieve more accurate sea ice concentration results, the ASI algorithm should be validated and improved. In this study, based on a data fusion method, the polarization difference in the 91 GHz band was modified using the polarization difference in the 19 GHz band sea ice concentration the 91 GHz band. The results obtained using this method can greatly reduce the error caused by atmosphere by effectively correcting the mixed pixel sea ice concentrations.

2 Data set

The SSMIS is a passive microwave radiometer launched aboard the Defense Meteorological Satellite Program (DMSP) F-16, F-17, and F-18 in 2003, 2006, and 2009. SSMIS increased from 7-channel and 4-frequency of SSM/I to 24 different frequency channels; therefore, it collects brightness temperature measurements at a number of different polarizations and frequencies (Li, 1996; IPCC, 2013; Hollinger, 1989). SSMIS data are obtained from the National Snow and Ice Data Center (NSIDC), which provides daily average Arctic brightness temperature images on a 25 km/pixel resolution grid in a polar stereographic projection (Tschudi et al., 2016).

SSMIS measures surface/atmospheric microwave brightness temperatures (TBs) at 19.35, 22.235, 37.0 and 91 GHz. The four frequencies are sampled in both horizontal and vertical polarizations (NSIDC, 2010). The sensor samples data at two different spatial intervals, the first at 25 km (for the 19, 23 and 37 GHz channels) and the second at 12.5 km (for the 91-GHz channel). At these intervals, the footprint from the 37 GHz channel typically overlaps with four or five neighboring footprints, while a footprint from the 19 GHz channel overlaps with seven to nine neighboring footprints. Hence, in gridded SSMIS data, such as the 25 km× 25 km grid used in the NSIDC data product, each observation is actually an average of a number of neighboring pixels in the raw data. In contrast, the sampling spacing for the 91 GHz channel is almost equal to the footprint dimensions (13 km×15 km); therefore, slight overlapping occurs between adjacent footprints in the gridded data. The radiometric characteristics of the specific SSMIS are shown in Table 1.

Table 1. Radiometric characteristics of the SSMIS

Frequency/GHz	Polarization	Along-track resolution/km	Cross-track resolution/km	Spatial sampling/km	Instrument noise/K
19.35	horizontal	69	43	25	0.42
19.35	vertical	69	43	25	0.45
22.235	horizontal	50	40	25	0.74
22.235	vertical	50	40	25	0.74
37.0	horizontal	37	28	25	0.38
37.0	vertical	37	28	25	0.37
91.665	horizontal	15	13	12.5	0.73
91.665	vertical	15	13	12.5	0.69

3 Algorithm

3.1 *Algorithm description*

The ASI algorithm is typically used to calculate sea ice concentration from high-frequency data. The advantage of the ASI algorithm is that it does not require additional data entry needed in the other 85 GHz algorithms (Kern, 2004) while still producing results similar to sea ice concentration by algorithms using other channels (Kern et al., 2003). However, like other high-frequency algorithms, it is susceptible to be interfered by surface water vapor, which causes performances degraded over ocean areas, and especially at the Marginal Ice Zone.

High-frequency data algorithms are often processed using weather filters. In general, most weather effects can be removed using two filters: Gradient Ratio (GR) (37/19) and GR (22/19). However, the weather filter assumes that GR values are positive for water, and close to zero or negative for ice. The weather filter simply removes the water that is misjudged as sea ice but does not change the mixed pixels for sea ice concentration. Therefore, to get high spatial resolution sea ice concentration results more accurately, we propose an enhanced ASI algorithm, which uses low-frequency data to correct high-frequency results.

3.2 *An enhanced ASI algorithm*

The ASI algorithm is based on the polarization difference (P) used to calculate the sea ice concentration (Svendsen et al., 1987).

$$P = T_{\mathrm{bv}} - T_{\mathrm{bh}}, \tag{1}$$

where T_{bv} and T_{bh} denote brightness temperatures at vertical and horizontal polarizations, respectively.

To calculate all sea ice concentrations from 0% to 100%, a third-order polynomial was chosen to fit 0% to 100% of the sea ice concentration as follows:

$$C = d_3P^3 + d_2P^2 + d_1P + d_0. \tag{2}$$

Assuming that point values for pure water and pure ice are known, they are expressed as P_0 and P_1, respectively. Then, by inserting them into the first derivative formula of Eq. (2), another two equations can be acquired.

Polarization differences on the ice surface are significantly smaller than those of open water. When the C approaches 0 and 1, the P becomes P_0 and P_1, respectively. As shown in Eq. (3), d_0, d_1, d_2 and d_3 can be calculated.

$$\begin{bmatrix} {P_0}^3 & {P_0}^2 & P_0 & 1 \\ {P_1}^3 & {P_1}^2 & P_1 & 1 \\ 3{P_0}^2 & P_1 & 1 & 0 \\ 3{P_1}^2 & 2P_1 & 1 & 0 \end{bmatrix} \cdot \begin{bmatrix} d_3 \\ d_2 \\ d_1 \\ d_0 \end{bmatrix} = \begin{bmatrix} 0 \\ 1 \\ -1.14 \\ -0.14 \end{bmatrix}. \quad (3)$$

These values of d_0, d_1, d_2 and d_3 are then be substituted into Eq. (2) to obtain the sea ice concentration (Kaleschke et al., 2001).

Based on SSM/I 85.5 GHz data, sea ice concentration is calculated as follows (Kaleschke et al., 2001):

$$C = 6.457\ 14 \times 10^{-6} P^3 - 6.052\ 56 \times 10^{-4} P^2 - 9.225\ 21 \times 10^{-3} P + 1.100\ 31. \quad (4)$$

Based on AMSR-E 89 GHz data, sea ice concentration is calculated as follows (Spreen et al., 2008):

$$C = 1.640 \times 10^{-5} P^3 - 1.618 \times 10^{-3} P^2 + 1.916 \times 10^{-2} P + 0.971\ 0. \quad (5)$$

In these expressions for sea ice concentration, values for d_0, d_1, d_2, and d_3 can be determined and the polarization differences calculated as long as appropriate data are used. Because SSMIS 91 GHz channel data is used in this study, and the properties of SSMIS 91 GHz and SSM/I 85.5 GHz are basically the same, so use Eq. (4) is selected for computing to sea ice concentration.

A large number of sample points from the 91 GHz and 19 GHz bands are selected and the polarization difference at each sample point is calculated. Then, the values are fitted to determine the relationship of the polarization difference between the 91 GHz and 19 GHz bands. Finally, using the matched datasets, we produce the following correction formula:

$$P' = d{P_{19}}^3 + c{P_{19}}^2 + bP_{19} + a. \quad (6)$$

where P_{19} is the 19 GHz polarization difference after resampling using the 91 GHz data and P' is the polarization difference in the modified 91 GHz. Variables a, b, c and d are the four modified parameters. Their values are –14.578, 2.214, -5.649×10^{-2}, and 5.200×10^{-4}, respectively. The Goodness of Fit for the revised formula is 0.97. The P' (modified polarization difference of 91 GHz) is substituted into Eq. (4), and the sea ice concentration obtained.

4 Results

4.1 *Comparative analysis of polarization differences*

To distinguish more intuitively between P (91 GHz polarization difference) and P' (modified 91 GHz polarization difference), we take the data from January 3, 2016 as an example; the 91 GHz polarization difference (P) and corrected 91 GHz polarization difference (P') for color images are shown in Figs 1a and b, respectively. By comparison, P values show more clutter in areas of open water and the layering is worse, which indicates more significant weather effects. The P' values are more uniform, especially over open water. Clear ring characteristics are observable, indicating the significant differences between P and P'. In Fig. 1a, most pixels in the two black rectangles in the lower right area of the frame are the same as those in the central area of the Arctic Ocean; however, pixels in this area should be seawater instead of sea ice, which shows the effect of weather on high frequency data. In Fig. 1b, after the polarization data have been corrected for the same area, these pixels become consistent with open ocean.

4.2 *Overall area validation analysis*

In general, due to the influence of weather, sea ice concentration results obtained from high-frequency data are often higher than those obtained from low-frequency data. Studies have shown that the overall sea ice area results obtained using the ASI algorithm are larger than those obtained with the NASA Team algorithm (Wang, 2009). The results obtained from SSMIS data are shown in Fig. 2. All three results have been processed with a weather filter. The total sea ice area obtained from the ASI, NASA Team, and enhanced ASI algorithm for January 3, 2016 are 11.406×10^6 km^2, 10.313×10^6 km^2, and 11.093×10^6 km^2, respectively. The enhanced ASI algorithm result is about 7% higher than that of the NASA Team algorithm, while the result of the ASI algorithm is

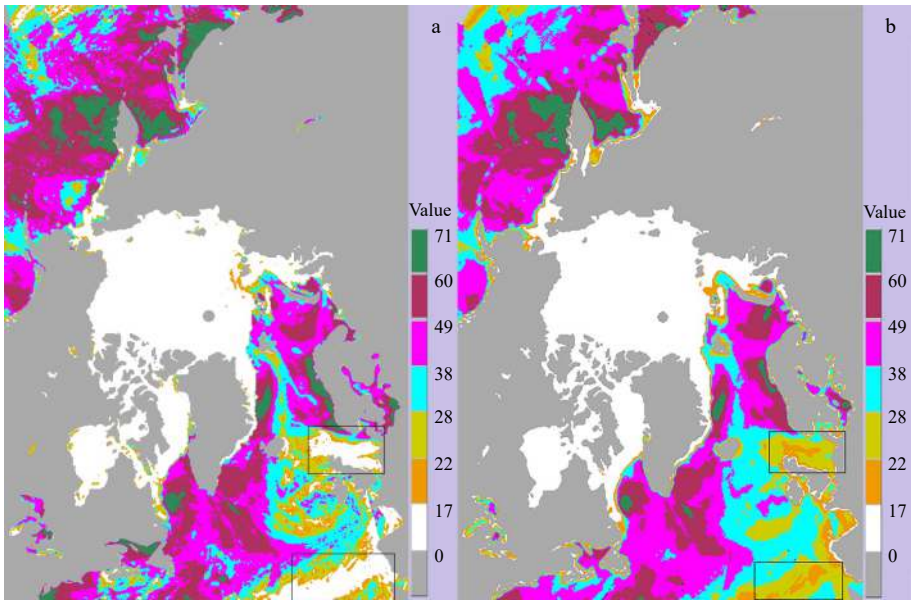

Fig. 1. Polarization difference: a. 91 GHz polarization difference (P) and b. corrected 91 GHz polarization difference (P').

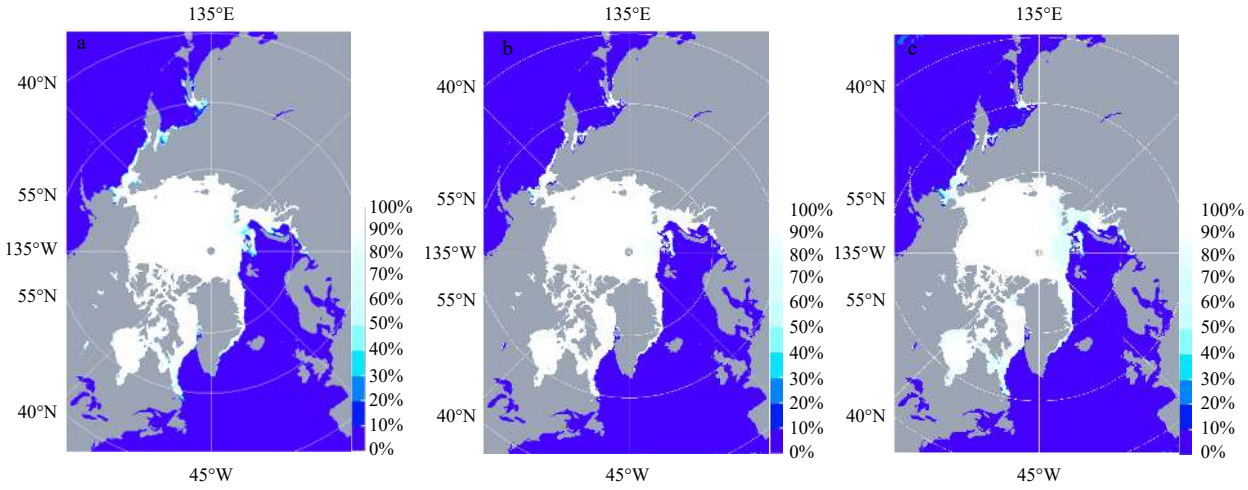

Fig. 2. Sea ice concentration results, from the ASI algorithm (a), enhanced ASI algorithm (b), and NASA Team algorithm (c).

9.6% higher than that of the NASA Team algorithm. The enhanced ASI algorithm results lies between those of the other two algorithms, which suggests that the enhanced ASI algorithm produces a reasonably accurate value for total sea ice. To verify the feasibility and accuracy of the enhanced ASI algorithm, the same date in January from 2008 to 2017 are used for statistical analysis, as shown in Table 2 and Fig. 3.

As described in Fig. 3, the sea ice area calculated using the enhanced ASI algorithm lies between the original ASI and NASA Team results. The differences shown in Table 2 indicate that the results from the enhanced ASI algorithm are higher than those from the NASA Team algorithm, with average errors of 6.531%. The enhanced ASI results are lower than ASI, with an average error of –2.155%. Generally, the enhanced ASI algorithm proposed in this study provides results closer to the ASI results and higher than NASA Team results in terms of total sea ice area.

4.3 *Comparative analysis of the marginal sea ice zone*

As shown in Figs 2a–c, the center of the Arctic Ocean was covered by sea ice on January 3, 2016 with an ice concentration

Table 2. Sea ice area results calculated from the three algorithms for the entire Arctic region

Date	Enhanced ASI/10^6 km^2	NASA Team/10^6 km^2	ASI/10^6 km^2	Enhanced ASI minus NASA Team/%	Enhanced ASI minus ASI/%
2008–01–03	11.999	11.307	12.161	5.767	–1.350
2009–01–03	12.120	11.232	12.233	7.326	–0.093
2010–01–03	11.882	10.892	12.027	8.332	–1.220
2011–01–03	11.382	10.630	11.902	6.607	–4.568
2012–01–03	12.245	11.353	12.425	7.284	–1.469
2013–01–03	11.814	11.349	12.352	3.936	–4.554
2014–01–03	12.174	11.523	12.344	5.347	–1.396
2015–01–03	11.856	11.096	12.023	6.410	–1.409
2016–01–03	11.093	10.313	11.406	7.031	–2.822
2017–01–03	11.108	10.301	11.404	7.265	–2.665
Average	11.767	10.000	12.028	6.531	–2.155

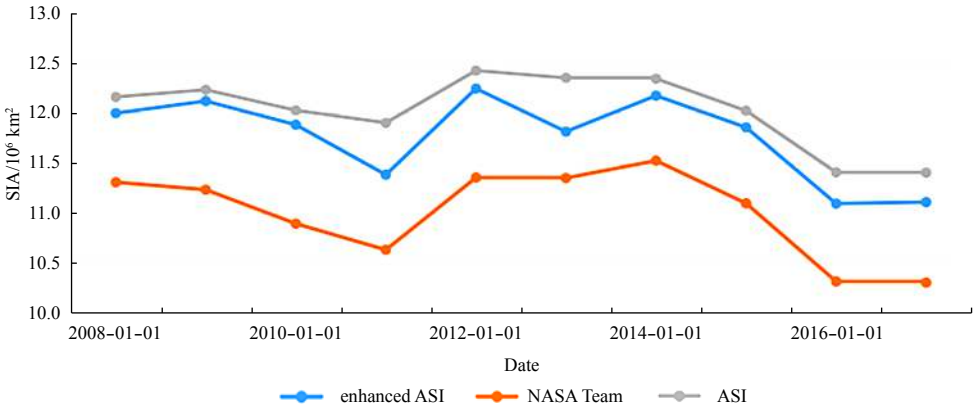

Fig. 3. Arctic sea ice area results for January 3 from 2008 to 2017.

greater than 0.95. The biggest difference between Figs 2a, b and c is in the ice near the coasts of Svalbard and Greenland. Compared to the other two algorithms, the ASI algorithm results are significantly higher NASA Team in the Marginal Ice Zone. To identify an explanation, the Marginal Ice Zone is extracted and the following results obtained. The sea ice area is 1.23×10^6 km^2 based on the ASI algorithm, while the results from the enhanced ASI and NASA Team algorithms are 1.05×10^6 and 0.863×10^6 km^2, respectively; the ASI and enhanced ASI results are 29.8% and 17.8% higher than that of the NASA Team result, respectively. Results from the three algorithms for the Marginal Ice Zone are shown in Fig. 4. Figure 4a shows the difference between ASI and NASA Team results, and Fig. 4b shows the difference between the enhanced ASI algorithm and NASA Team results. On average, the ASI algorithm results are 0.17 higher than that of NASA Team, with a standard deviation of 0.15. On average, the enhanced ASI algorithm results are 0.15 higher than that of NASA Team, with a standard deviation of 0.10. In summary, the sea ice concentration obtained using the ASI algorithm is larger than that of NASA Team. The enhanced ASI algorithm results are closer to those using the NASA Team algorithm, with much smaller differences in concentration.

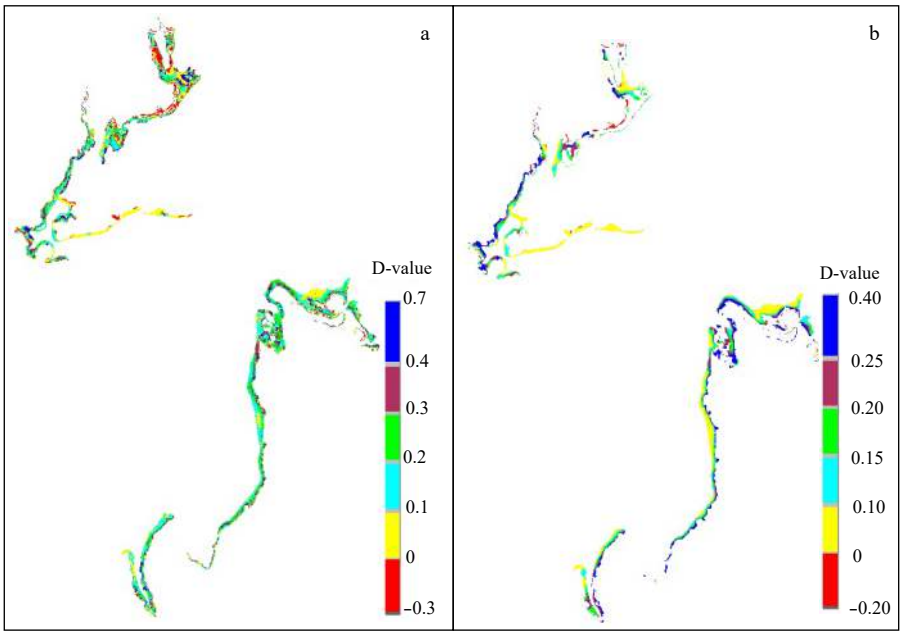

Fig. 4. D-values for ASI algorithm minus NASA Team algorithm (a) and enhanced ASI algorithm minus NASA Team algorithm (b).

4.4 *Subarea validation analysis*

To compare the accuracy of the enhanced ASI algorithm, the sea ice area and concentration are analyzed in different regions. We selected the central region of the Arctic Ocean and found that the enhanced ASI and the other results show no large difference in sea ice area and average concentration. Next, we chose the small zone between Novaya Zemlya, Severnaya Zemlya, and Franz Josef Land to compare and analyze, where the specific location is shown in the red box in Fig. 5. Using the January 3, 2012 data for illustration, the distribution of sea ice concentration is shown in Fig. 6. Furthermore, a statistical analysis of data from January 3, from 2012 to 2015, is provided in Table 3. As shown in Fig. 6, the average sea ice concentration results from the enhanced ASI algorithm for January 3, 2012 are lower than the ASI results and higher than the NASA Team results. From the statistics in Table 3, the enhanced ASI results always lie between the other two results for both sea ice area and concentration.

5 Discussion

The enhanced ASI algorithm has some limitations. For example, values for pure water and pure ice will change with the seasons and depend on geographical variations. We obtained these values using a statistical sample point correction equation for winter Arctic sea ice. This exercise produces concentration results more accurately than if we had used a data selection for other regions or seasons.

In verification, we only use the results from the other two algorithms based on microwave data to cross-compare. Because

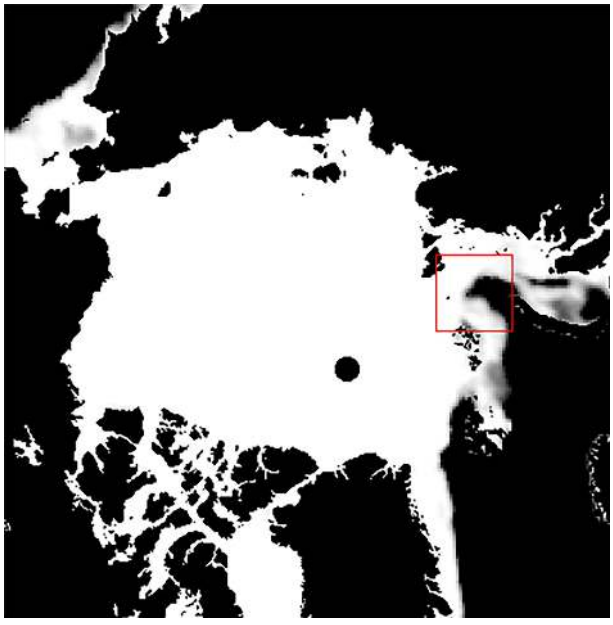

Fig. 5. Location of subarea validation analysis.

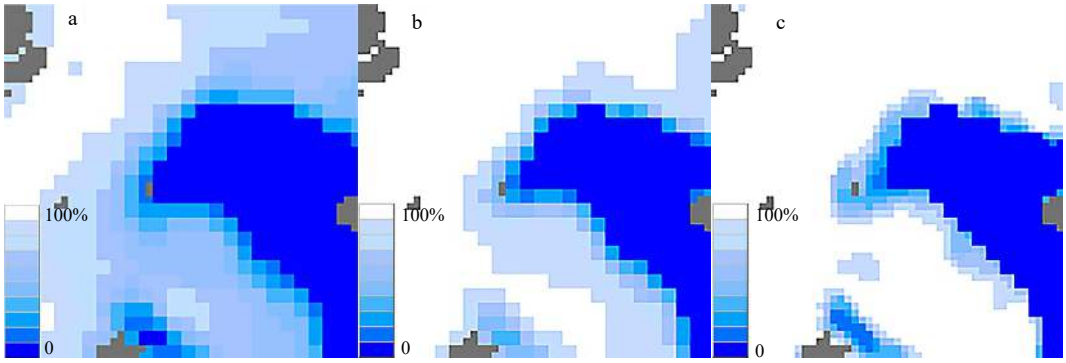

Fig. 6. Sea ice concentration results for a small region, from the NASA Team algorithm (a), enhanced ASI (b), and ASI algorithm (c).

Table 3. Sea ice area and concentration results calculated from the three algorithms for the subarea

Date	Enhanced ASI /10^6 km^2	Enhanced ASI concentration	NASA Team /10^6 km^2	NASA Team concentration	ASI /10^6 km^2	ASI concentration
2012–01–03	0.276 8	0.901 1	0.212 5	0.733 6	0.289 7	0.933 7
2013–01–03	0.288 5	0.931 8	0.257 6	0.831 9	0.304 2	0.925 5
2014–01–03	0.343 7	0.972 7	0.338 8	0.958 8	0.352 5	0.984 8
2015–01–03	0.367 4	0.984 6	0.355 8	0.953 7	0.385 3	0.987 7

optical data are influenced by weather, the cloud distribution should be considered, which is not suitable for large area and long-time series sea ice retrievals. There are some differences between the radar data and SSMIS data according to the satellite platform, which produces some uncertainty in the sea ice retrieval results. Of course, using optical data has obvious advantages in validating local small areas, but weather conditions in the verification area need to be determined in advance to meet the calculation conditions.

6 Conclusions

In this study, SSMIS data from 2008 to 2017 were used to calculate Arctic Sea ice concentrations. The enhanced ASI algorithm is developed based on the ASI algorithm by using the 19 GHz polarization difference to modify the 91 GHz polarization difference. We used NASA Team and ASI algorithms to test the enhanced ASI algorithm. The results of three algorithms show that the sea ice areas calculated from the enhanced ASI algorithm are lower than those of the ASI and higher than those of the NASA Team algorithm. Using data of SSMIS from January 3, 2016, the sea ice concentration calculated from the enhanced ASI algorithm is lower than the result calculated from the ASI algorithm in the marginal ice zone, with a difference in sea ice area of 15%. Sea ice concentrations above 0.15 calculated using enhanced ASI algorithm are 28.6% less the same concentration level calculated using the ASI algorithm. In the marginal ice zone, the enhanced ASI algorithm significantly changes the ice concentration of mixed pixels, which by reducing the impact of weather on high-frequency data.

Acknowledgements

We thank the anonymous reviewers for their time and effort, which significantly improve the manuscript.

References

Andersen S, Tonboe R, Kaleschke L, et al. 2007. Intercomparison of passive microwave sea ice concentration retrievals over the high-concentration Arctic sea ice. Journal of Geophysical Research: Oceans, 112(C8): 207–220

Budikova D. 2009. Role of arctic sea ice in global atmospheric circulation: a review. Global and Planetary Change, 68(3): 149–163, doi: 10.1016/j.gloplacha.2009.04.001

Comiso J C. 1986. Characteristics of arctic winter sea ice from satellite multispectral microwave observations. Journal of Geophysical Research: Oceans, 91(C1): 975–994, doi: 10.1029/JC091iC01p00975

Comiso J C. 1995. SSM/I sea ice concentrations using the bootstrap algorithm. NASA Goddard Space Flight Center Ref. Publication, No. 1380. Washington: National Aeronautics and Space Administration

Gabarro C, Turiel A, Elosegui P, et al. 2017. New methodology to estimate Arctic sea ice concentration from SMOS combining brightness temperature differences in a maximum-likelihood estimator. The Cryosphere, 11(4): 1987–2002, doi: 10.5194/tc-11-1987-2017

Hollinger J P. 1989. DMSP Special Sensor Microwave/Imager Calibration/Validation. Final Report, Vol. I. Washington DC: Space Sensing Branch, Naval Research Laboratory

IPCC. Climate Change 2013: The Physical Science Basis. Contribution of Working Group I to the Fifth Assessment Report of the Intergovernmental Panel on Climate Change. New York: Cambridge University Press

Kaleschke L, Lüpkes C, Vihma T, et al. 2001. SSM/I sea ice remote sensing for mesoscale ocean-atmosphere interaction analysis. Canadian Journal of Remote Sensing, 27(5): 526–537, doi: 10.1080/07038992.2001.10854892

Kern S. 2004. A new method for medium-resolution sea ice analysis using weather-influence corrected Special Sensor Microwave/Imager 85 GHz data. International Journal of Remote Sensing, 25(21): 4555–4582, doi: 10.1080/01431160410001698898

Kern S, Heygster G. 2001. Sea-ice concentration retrieval in the antarctic based on the SSM/I 85.5 GHz polarization. Annals of Glaciology, 33(1): 109–114

Kern S, Kaleschke L, Clausi D A. 2003. A comparison of two 85-GHz SSM/I ice concentration algorithms with AVHRR and ERS-2 SAR imagery. IEEE Transactions on Geoscience and Remote Sensing, 41(10): 2294–2306, doi: 10.1109/TGRS.2003.817181

Kern S, Rösel A, Pedersen L T, et al. 2016. The impact of melt ponds on summertime microwave brightness temperatures and sea-ice concentrations. The Cryosphere, 10(5): 2217–2239, doi: 10.5194/tc-10-2217-2016

Korosov A A, Rampal P, Pedersen L T, et al. 2018. A new tracking al-

gorithm for sea ice age distribution estimation. The Cryosphere, 12(6): 2073–2085, doi: 10.5194/tc-12-2073-2018

Li Peiji. 1996. The arctic sea ice and climate change. Journal of Glaciology and Geocryology (in Chinese), 18(1): 72–80

Markus T, Cavalieri D J. 2000. An enhancement of the NASA team sea ice algorithm. IEEE Transactions on Geoscience and Remote Sensing, 38(3): 1387–1398, doi: 10.1109/36.843033

NSIDC. 2010. Special Sensor Microwave/Imager (SSM/I) and Special Sensor Microwave Imager Sounder (SSMIS) Global Gridded Products. Silver Spring: National Environmental Satellite, Data, and Information Service (NESDIS), NOAA

Schmidtko S, Heywood K J, Thompson A F, et al. 2014. Multidecadal warming of Antarctic waters. Science, 346(6214): 1227–1231, doi: 10.1126/science.1256117

Spencer R W, Goodman H M, Hood R E. 1989. Precipitation retrieval over land and ocean with the SSM/I: identification and characteristics of the scattering signal. Journal of Atmospheric and Oceanic Technology, 6(2): 254–273, doi: 10.1175/1520-0426(1989)006<0254:PROLAO>2.0.CO;2

Spreen G, Kaleschke L, Heygster G. 2008. Sea ice remote sensing using AMSR-E 89-GHz channels. Journal of Geophysical Research: Oceans, 113(C2): C02S03

Su Jie, Hao Guanghua, Ye Xinxin, et al. 2013. The experiment and validation of sea ice concentration AMSR-E retrieval algorithm in polar region. Journal of Remote Sensing (in Chinese), 17(3): 495–513

Svendsen E, Matzler C, Grenfell T C. 1987. A model for retrieving total sea ice concentration from a spaceborne dual-polarized passive microwave instrument operating near 90 GHz. International Journal of Remote Sensing, 8(10): 1479–1487, doi: 10.1080/01431168708954790

Swift C, Cavalieri D. 1985. Passive microwave remote sensing for sea ice research. Eos, Transactions American Geophysical Union, 66(49): 1210–1212, doi: 10.1029/EO066i049p01210

Tschudi M, Fowler C, Maslanik J, et al. 2016. Polar Pathfinder Daily 25 km EASE-Grid Sea Ice Motion Vectors, Version 3. Boulder, Colorado, USA: NASA National Snow and Ice Data Center Distributed Active Archive Center, doi: https://doi.org/10.5067/O57VAIT2AYYY

Wang Huanhuan. 2009. Multiyear ice retrieval using passive microwave remote sensing radiometer AMSR-E 89GHz data (in Chinese) [dissertation]. Qingdao: Ocean University of China

Ye Yufang, Heygster G, Shokr M. 2016. Improving multiyear ice concentration estimates with reanalysis air temperatures. IEEE Transactions on Geoscience and Remote Sensing, 54(5): 2602–2614, doi: 10.1109/TGRS.2015.2503884

Zhang Shugang. 2012. Sea ice concentration algorithm and study on the physical process about sea ice and melt-pond change in Central Arctic (in Chinese) [dissertation]. Qingdao: Ocean University of China

Zhang Xiang, Wang Zhenzhan, Shen Hua. 2012. A sea ice concentration algorithm based on HY-2 scanning radiometer data. Remote Sensing Technology and Application (in Chinese), 27(6): 912–918